

of the two methods. The solution to the self-consistent field equations was an eigenstate characterized by a particular direction θ [Eq. (30)]. However, if the mirror is highly anisotropic the wave suffers a significant amount of rotation upon reflection [cf. Eq. (27)], so a single direction of polarization is, in this case, not an adequate kind of description. If the anisotropy is weak, the reflection rotation is small, and it then becomes a good approximation to say that the wave is always in one particular direction.

Lasers having mirrors which show a weak loss anisotropy have been studied experimentally,¹⁴⁻¹⁶ but no studies have been reported for the case of a substantial loss anisotropy. If observations were to be made for this latter case and compared to the results presented here, it should be remembered that the wave which is described in Eq. (1) is the wave incident upon the anisotropic mirror. To find the transmitted wave one must take account of the transmission matrix for the anisotropic mirror (assuming, as is most likely, that the output is taken there).

In summary, then, we have considered in detail a centrally tuned laser subject to an axial magnetic field and having one end mirror which shows an x - y -type of loss anisotropy. It was found that the behavior of the

frequency-locked modes of linear polarization is to a large extent independent of the complex details of the nonlinear interactions, with the result that the mathematics required to describe these modes is relatively simple.²¹ Thus, a consideration of these modes is especially appropriate to the purpose of illustrating through a concrete example the differences between two theoretical bases, namely, (a) application of the resonance condition for a round-trip pass, and (b) the use of the self-consistent field equations with distributed loss. In general, the former method (a) should be used, although the differences between the two become negligible in the limit of small asymmetries. In the example considered here, the theory predicts, in the case of mirrors with a strong loss anisotropy, some new features which have yet to be observed.

²¹ This mathematical simplicity, it should be noted, derives from the fact that the symmetry relations (12) allow for a rather full treatment of the eigenvalue problem; in particular, the solutions for the frequency of oscillation and the eigenstate of polarization do not depend on the details of the nonlinearities, which are contained in the susceptibility χ . Thus for the frequency-locked modes of linear polarization the simplicity of their physical behavior is reflected in the mathematics. The situation would, of course, not be so simple for other configurations (e.g., two frequency operation, detuning of the cavity from line center, the inclusion of phase anisotropies).

Spin-Lattice Relaxation of F Centers in Alkali Halides: Theory and Optical Measurements to 50 kG*

H. PANEUCCI† AND L. F. MOLLENAUER

Department of Physics, University of California, Berkeley, California 94720

(Received 23 September 1968)

We have measured the ground-state spin-lattice relaxation of F centers in KBr and KI over the range of magnetic field from 0 to 50 kG, and at the temperature of 1.6°K. Essentially continuous measurement over this large field range was made possible by a detection technique in which the magnetic circular dichroism of the optical absorption band was monitored. In the range 10 to 50 kG, the relaxation rate is predominantly that of single F centers. Here, the field dependence of the relaxation rate followed very closely a curve of the form $(AH^3 + BH^5)\coth(g\beta H/2KT)$. The first term represents a mechanism involving phonon modulation of the hyperfine contact interaction with neighboring nuclei, and is the larger term for $H_0 \lesssim 25$ kG. The second term is due to relaxation via the Kronig-Van Vleck process. A theoretical evaluation of that part of the rate due to the hyperfine mechanism has produced close agreement with experimental results. In the evaluation, the interaction with the second shell of nuclei (halogens) was found to be of greatest importance for KBr and KI.

I. INTRODUCTION

AT very low temperatures, where the Raman process is frozen out, spin-lattice relaxation of F centers in alkali halides takes place by the direct process.¹ In its ground state, the F -center electron may

be approximately described by an s -type wave function which spreads out over many lattice sites. At all but the highest fields, a relaxation process by way of modulation of the hyperfine interaction may predominate over the common mechanism of modulation of the crystal field, which for an s -type electron should be very small. From measurements of field dependence

* Supported in part by the U. S. Atomic Energy Commission. Report No. UCB-34P20-136.

† Visiting Research Fellow of the Consejo Nacional de Investigaciones Científicas y Técnicas, Argentina.

¹ For a good collection of papers, see *Spin-Lattice Relaxation in*

Ionic Solids, edited by A. A. Manenkov and R. Orbach (Harper and Row, New York, 1966).

of T_1 in KCl by Feldman, Warren and Castle,² it was concluded that the hyperfine mechanism was indeed the major one. A further test of the importance of this mechanism would be provided by similar measurements on other alkali halides having the same F center structure. For this purpose we have chosen KBr and KI.

It is apparent from the discrepancies in the values of T_1 measured by different authors²⁻⁵ that it is difficult to obtain the true relaxation rates for pure and isolated F centers at low fields ($H_0 \lesssim 10$ kG). However, the authors of Ref. 2 were able to produce KCl samples of extremely good quality which gave reproducible and long values for T_1 . In Ref. 6, the same authors studied what they call extrinsic effects and found them mainly due to relaxation via clusters of F centers. This effect of clusters was found to become less important as the magnetic field was increased, and the relaxation rates approached the values for isolated centers at the highest fields used, about 10 kG. A theoretical analysis of the cluster effect was given by Glinchuk *et al.*,⁷ and also indicates that the effect of the clusters should become relatively unimportant at high fields, especially at low F -center concentration.

According to the above discussion, it is necessary, or at least desirable, to measure T_1 at high fields ($H_0 > 10$ kG) and low F -center concentration in order to be sure that one is measuring the true values for the isolated F center. Under these conditions of high field and low concentration, the standard microwave techniques are very difficult or impossible to apply, both because of the high resonance frequencies involved, and because of sensitivity requirements. Therefore, for our measurements on KBr and KI we have chosen an optical technique of high sensitivity which is independent of microwave apparatus and which is very easily adaptable to varying the field, in contrast to microwave methods. By monitoring the magnetic circular dichroism of the optical absorption band, we have a direct measure of the electron-spin polarization in the F -center ground state. A burst of optical pumping light provides the necessary displacement away from thermal equilibrium to allow observation of the relaxation. This method provided excellent signal-to-noise ratio for F -center concentrations considerably less than 10^{16} /cc. It should be mentioned here that our detection scheme is similar to that used by Karlov

*et al.*⁸ in their studies of the F center in KBr; however, the authors of Ref. 8 limited their measurements of T_1 to the field range 1 to 9 kG, nor were their measurements entirely independent of microwave sources.

The experimental results for KBr and KI obtained by the above method have yielded a field dependence for the relaxation rate of the form $(AH^3 + BH^6) \times \coth g\beta H / 2KT$ for fields in excess of 5 kG. The first term corresponds to that expected for the hyperfine modulation mechanism, and is the predominant term for $H_0 \lesssim 25$ kG. The second term in the field dependence is that expected for relaxation via the Kronig-Van Vleck mechanism, and is of major importance only for the highest fields ($H_0 \gtrsim 25$ kG).

We have used a Gourary and Adrian type wave function,⁹ orthogonalized to the core orbitals of the ions in the first two shells to estimate theoretically the relaxation rates for the hyperfine mechanism. As a result we arrived at an expression containing only known parameters, such as the hyperfine constants for the different alkali halides determined from ENDOR experiments.¹⁰ In this way we can explain the relative size of the relaxation rates as well as the absolute values for KBr, KI and also KCl, which is included for comparison. Furthermore, we show that for KBr and KI, interaction with the second shell of nuclei (halogens) is of even greater importance than that with the first (alkali) shell.

II. THEORY OF SPIN-LATTICE RELAXATION BY MODULATION OF THE HYPERFINE INTERACTION

The different mechanisms which may lead to an energy exchange between the electron spin system and the lattice vibrations, and thus to the relaxation of the z component of the magnetization are: (1) phonon modulation of dipole-dipole coupling between the paramagnetic centers, (2) phonon modulation of the crystal-field interaction with the electron spin which takes place through the spin-orbit coupling and (3) phonon modulation of the hyperfine interaction of the electrons with the nuclei of neighboring ions.

The first, discussed by Waller,¹¹ yields the same behavior with field as found experimentally here for the F centers in KI and KBr. On the other hand, the Waller mechanism will exhibit a strong concentration dependence, and leads to very large values of T_1 for the low concentrations studied here; both predictions are in contradiction with the experimental results. Thus, this mechanism may be omitted from consideration.

² D. W. Feldman, R. W. Warren, and J. G. Castle, Phys. Rev. **135**, A470 (1964).

³ G. A. Noble and J. J. Markham, Bull. Am. Phys. Soc. **5**, 419 (1960).

⁴ W. D. Ohlsen and D. F. Holcomb, Phys. Rev. **126**, 1953 (1962).

⁵ J. Mort, F. Lüty, and F. C. Brown, Phys. Rev. **137**, A566 (1965).

⁶ R. W. Warren, D. W. Feldman, and J. G. Castle, Phys. Rev. **136**, A1347 (1964).

⁷ M. D. Glinchuk, V. G. Grachev, and M. F. Dergin, Fiz. Tverd. Tela **8**, 3354 (1967) [English transl.: Soviet Phys.—Solid State **8**, 2678 (1967)].

⁸ N. V. Karlov, J. Margerie, and Y. Merle-D'Aubigné, J. Phys. (Paris) **24**, 717 (1963).

⁹ B. S. Gourary and F. J. Adrian, Phys. Rev. **105**, 1180 (1957).

¹⁰ H. Siedel, Z. Physik **165**, 218 (1961).

¹¹ I. Waller, Z. Physik **79**, 370 (1932).

The second mechanism, introduced by Kronig¹² and independently by Van Vleck,¹³ leads to a $H^5 \times \coth(g\beta H/2KT)$ dependence of the rate when applied to Kramer's conjugate states such as the *F*-center ground state in alkali halides. The results of this work show such a field dependence at the very highest fields for KBr and KI. We defer further discussion of this mechanism until a later section in which we compare the experimental results with an expression for the relaxation rate calculated by Kronig.¹²

Thus, the only mechanism left for calculation is that of the modulation of hyperfine interaction. We shall restrict our treatment to the contact or isotropic hyperfine interaction, and neglect the much smaller anisotropic terms. Further, we will be concerned only with a region of temperature sufficiently low such that only the direct process is involved.

We should mention that Deigen and Zevin¹⁴ have employed this mechanism to calculate the relaxation rate for KCl. However, their treatment, which requires considerably more complex calculations, yields results less accurate than those of the simpler theory given below. Furthermore their theory is limited to the six nearest neighbors, and thus it cannot explain the differences among the various potassium halides.

For the interaction between the *F*-center spin and the *m*th neighboring nucleus we take the contact hyperfine operator:

$$\mathcal{H} = a_m \mathbf{I}_m \cdot \mathbf{S} |\psi(\mathbf{r}_m)|^2, \quad (1)$$

where $a_m = 8\pi/3\mu_0\mu_I$, and where $\psi(\mathbf{r}_m)$ is the *F*-center wave function evaluated at the site of the *m*th nucleus. Thus, at sufficiently high fields, the splittings will be given by

$$h\nu_m = \frac{1}{2} a_m |\psi(\mathbf{r}_m^0)|^2. \quad (2)$$

The relaxation mechanism is based upon the fact that the lattice vibrations make \mathbf{r}_m , and hence \mathcal{H} , functions of time. For convenience, we write the nuclear coordinate $\mathbf{r}_m = \mathbf{r}_m^0 + \mathbf{u}_m(t)$, where \mathbf{r}_m^0 is the equilibrium position and $\mathbf{u}_m(t)$ the displacement from equilibrium. Similarly, we write $\mathbf{r}_l = \mathbf{r}_l^0 + \mathbf{u}_l(t)$ for the *F* center. The relationship among the various coordinates is shown in Fig. 1. Furthermore, it is convenient to define

$$\mathbf{u}_{lm} = \mathbf{u}_l - \mathbf{u}_m. \quad (3)$$

It will be shown later that for the $\psi(\mathbf{r}_m)$ assumed here, $\psi(\mathbf{r}_m)$ is a function only of the distance r_{lm} between the *F* center and the nucleus *m*. Thus, we are justified in expanding \mathcal{H} in the following form:

$$\mathcal{H}(t) = a_m \mathbf{I}_m \cdot \mathbf{S} |\psi(\mathbf{r}_m)|^2 + a_m \mathbf{I}_m \cdot \mathbf{S} \nabla |\psi(\mathbf{r}_m)|^2 \cdot \mathbf{u}_{lm}(t) + \dots = \mathcal{H}_0 + \mathcal{H}_{\text{pert}}(t).$$

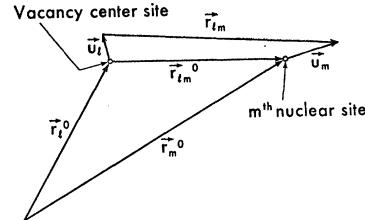


FIG. 1. Coordinate system defining displacement of the *m*th nucleus relative to the *F* center.

$\mathcal{H}_{\text{pert}}(t)$ in the above is restricted to terms linear in the \mathbf{u}_{lm} , since we are interested only in processes involving single phonons. To describe the interaction with phonons, we must write the \mathbf{u}_l and the \mathbf{u}_m in terms of normal coordinates, following Waller,¹¹

$$\mathbf{u}_l = \sum_k \sum_{j=1}^3 [a_{kj} \cos(\mathbf{k} \cdot \mathbf{r}_l) + b_{kj} \sin(\mathbf{k} \cdot \mathbf{r}_l)] \hat{e}_{kj},$$

where \hat{e}_{kj} is a unit vector describing the polarization of the phonon of wave vector \mathbf{k} . Thus, in terms of the normal coordinates, $\mathcal{H}_{\text{pert}}$ becomes

$$\mathcal{H}_{\text{pert}} = a_m \mathbf{I}_m \cdot \mathbf{S} \sum_k \sum_j [a_{kj} \{ \cos \mathbf{k} \cdot \mathbf{r}_l - \cos \mathbf{k} \cdot \mathbf{r}_m \} + b_{kj} \{ \sin \mathbf{k} \cdot \mathbf{r}_l - \sin \mathbf{k} \cdot \mathbf{r}_m \}] \hat{e}_{kj} \cdot \nabla |\psi(\mathbf{r}_m)|^2. \quad (4)$$

Each term in the above summation leads to an independent process in which a phonon is created (or destroyed), of the type $M_S = \frac{1}{2}$, $M_m, n_{kj} \rightarrow M_S = -\frac{1}{2}$, $M_m + 1, n_{kj} + 1$, where n_{kj} is the number of phonons of propagation vector \mathbf{k} and polarization vector \mathbf{j} . The transition probability for such a process is given by

$$\frac{1}{\hbar^2} | \langle -\frac{1}{2}, M_m, n_{kj} | a_m \mathbf{I}_m \cdot \mathbf{S} a_{kj} (\cos \mathbf{k} \cdot \mathbf{r}_l - \cos \mathbf{k} \cdot \mathbf{r}_m) \times \hat{e}_{kj} \cdot \nabla |\psi(\mathbf{r}_m)|^2 | \frac{1}{2}, M_m + 1, n_{kj} + 1 \rangle |. \quad (5)$$

The total transition rate will be given by an appropriate sum of terms like Eq. (5) above.

To facilitate calculation of the individual probabilities, we split Eq. (5) into two factors:

$$| \langle -\frac{1}{2}, M_m | a_m \mathbf{I}_m \cdot \mathbf{S} | \frac{1}{2}, M_m + 1 \rangle |^2 = \frac{1}{4} a_m^2 (I_m + M_m + 1) (I_m - M_m), \quad (6a)$$

and

$$\begin{aligned} & | \langle n_{kj} + 1 | a_{kj} (\cos \mathbf{k} \cdot \mathbf{r}_l - \cos \mathbf{k} \cdot \mathbf{r}_m) \hat{e}_{kj} \cdot \nabla |\psi(\mathbf{r}_m)|^2 | n_{kj} \rangle |^2 \\ &= \left| \sum_{i=1}^3 \hat{e}_{kj} \cdot \hat{l}_i \nabla_i |\psi|^2 (\cos \mathbf{k} \cdot \mathbf{r}_l - \cos \mathbf{k} \cdot \mathbf{r}_m) \times \langle n_{kj} + 1 | a_{kj} | n_{kj} \rangle \right|^2 \\ &= \left[\frac{\kappa(n_{kj} + 1)}{2\pi\nu_{kj}} \right] \{ [\cos \mathbf{k} \cdot \mathbf{r}_l - \cos \mathbf{k} \cdot \mathbf{r}_m] \times \sum_i \hat{e}_{kj} \cdot \hat{l}_i \nabla_i |\psi|^2 \}^2, \quad (6b) \end{aligned}$$

¹² R. de L. Kronig, *Physica* **6**, 33 (1939).

¹³ J. H. Van Vleck, *Phys. Rev.* **57**, 426 (1940).

¹⁴ M. F. Deigen and V. Ya. Zevin, *Zh. Eksperim. i Teor. Fiz.* **39**, 1126 (1960) [English transl.: *Soviet Phys.—JETP* **12**, 785 (1961)].

where the \hat{l}_i are unit vectors in the x , y , and z directions which have been introduced to facilitate the summation over i , where $\kappa = \hbar/4\pi M$, and M is the total mass of the crystal.

To sum the probabilities we first bring together the cos and sin terms for a given k and j :

$$(\cos \mathbf{k} \cdot \mathbf{r}_l - \cos \mathbf{k} \cdot \mathbf{r}_n)^2 + (\sin \mathbf{k} \cdot \mathbf{r}_l - \sin \mathbf{k} \cdot \mathbf{r}_m)^2 \cong (\mathbf{k} \cdot \mathbf{r}_{lm})^2,$$

where we have made use of the fact that $\mathbf{k} \cdot \mathbf{r}_{lm} \ll 1$ since we are considering only low-frequency acoustic phonons. We then have for the sum of the squares of the matrix elements

$$\sum_{\mathbf{k}} \sum_j \frac{\kappa(n_{kj}+1)}{2\pi\nu_{kj}} (\mathbf{k} \cdot \mathbf{r}_{lm})^2 \left[\sum_i (\hat{e}_{kj} \cdot \hat{l}_i)^2 (\nabla_i |\psi|^2)^2 + \dots \right], \quad (7)$$

where the dots stand for terms that will average to zero. To evaluate the sum over k and j we make use of the fact that we are interested only in those values of \mathbf{k} for which $|\mathbf{k}| = \nu/v = g\beta H_0/v$, where v is the speed of sound. For simplicity, we have assumed a single value of v , when in fact v is somewhat dependent upon the propagation direction and polarization. We then replace the dot products in Eq. (6) by their average over-all polarization and propagation directions, and multiply by $3\gamma(\nu)$, where $\gamma(\nu)$ is the density of phonon modes:

$$\gamma(\nu) = 4\pi V(\nu^2/v^3).$$

In the above, V is the total volume of the crystal. Thus, over a unit frequency interval, the sum in Eq. (7) above becomes

$$\frac{\hbar}{6\pi\rho} \frac{1}{\nu^5} (\bar{n}_\nu + 1) (r_{lm})^2 \sum_i [\nabla_i |\psi|^2]^2, \quad (8)$$

where ρ is the mass density and \bar{n}_ν is the phonon-occupation index for temperature T .

Also in the summation of probabilities we must average Eq. (6a) over all possible initial-spin projections M_m , weighted by the probability of the initial-spin state. Thus, we obtain

$$\frac{1}{4} a_m^2 \sum_{-I_m}^{I_m} \frac{(I_m + M_m + 1)(I_m - M_m)}{2I_m + 1} = \frac{1}{6} a_m^2 I_m(I_m + 1). \quad (9)$$

Combining Eqs. (8) and (9), and multiplying by N_s , the number of (equivalent) nuclei in the s th shell surrounding the F center, we obtain for the total transition rate W_{+-} for a spin flip down due to interaction with the s th shell:

$$(W_{+-})_s = \frac{2\hbar}{9\rho} \frac{\nu^3}{\nu^5} (\bar{n}_\nu + 1) I_s(I_s + 1) \nu_s^2 \times N_s (r_{lm})^2 \sum_i \frac{[\nabla_i |\psi|^2]^2}{|\psi|^4}. \quad (10)$$

In Eq. (10) we have used Eq. (2) to replace a_s with its

equivalent in terms of the experimentally measured hyperfine frequencies ν_s .

If we write Eq. (10) above as $W_{+-} = K(\bar{n}_\nu + 1)$, then $W_{-+} = K\bar{n}_\nu$. From the rate equations¹ it can then be shown that the total relaxation rate due to interaction with the s th shell is

$$(1/T_1)_s = K \coth(\hbar\nu/2KT). \quad (11)$$

To obtain an expression for $(1/T_1)_s$ which may be compared with experiment, we have only to make a theoretical calculation of the final factor in Eq. (10) containing $\nabla |\psi|^2$; all the other parameters in Eq. (10) are well known. We shall use the following wavefunction for the F electron:

$$\psi = \frac{1}{N} \sum_{m,\alpha} \varphi_F - \langle \varphi_F | \varphi_{m,\alpha} \rangle \varphi_\alpha, \quad (12)$$

where N is a normalization factor, and

$$\varphi_F = A(a/\eta r) e^{-\eta r/a} \quad (13)$$

is the type-III Gourary and Adrian wave function⁹ from the point-lattice approximation; here a is the (smallest) interionic distance and η is a variational parameter. Thus, Eq. (12) represents the F -center wave function orthogonalized to all the orbitals $\psi_{m\alpha}$ of all the neighbor ions m in the first and second shells.

The overlap integrals $\langle \varphi_F | \varphi_{m\alpha} \rangle$ can be approximated¹⁵ by

$$\langle \varphi_F | \varphi_{m\alpha} \rangle \cong \varphi_F(r_{lm}) \int \varphi_{m\alpha} d\tau = \varphi_F(r_{lm}) \Gamma_{m\alpha}, \quad (14)$$

for the s -type ion core wave functions which give a contribution to $|\psi|^2$. The quantity is a constant with respect to position of the nucleus m .

In calculating $\nabla_i |\psi|^2$ we first notice that the electron density at the m th nucleus depends only upon its distance r_{lm} from the center of the vacancy; this is valid in the approximation where we ignore the overlap between the core orbitals of different ions. Thus,

$$\sum_i (\nabla_i |\psi|^2)^2 = \left(\frac{d|\psi|^2}{dr_{lm}} \right)^2. \quad (15)$$

Furthermore, when the right-hand side of Eq. (12) is squared, it has been shown¹⁶ that the most relevant contribution to $|\psi|^2$ comes from the terms involving $|\varphi_{m\alpha s}|^2$. Accordingly, we write

$$|\psi(r_{lm})|^2 \cong \frac{1}{N^2} \sum_{\alpha s} \langle \varphi_F(r_{lm}) | \varphi_{m\alpha s} \rangle^2 |\varphi_{m\alpha s}^{(0)}|^2 = \frac{1}{N^2} |\varphi_F(r_{lm})|^2 \sum_{\alpha s} \Gamma_{m\alpha s}^2 |\varphi_{m\alpha s}^{(0)}|^2 K |\varphi_F(r_{lm})|^2. \quad (16)$$

¹⁵ B. S. Gourary and F. J. Adrian, in *Solid State Physics*, edited by F. Seitz and D. Turnbull (Academic Press Inc., New York, 1960), Vol. 10, p. 246.

¹⁶ W. E. Blumberg and T. E. Das, *Phys. Rev.* **110**, 647 (1958).

Then

$$\frac{d}{dr_{lm}} |\psi(r_{lm})|^2 = K \frac{d}{dr_{lm}} |\varphi_F(r_{lm})|^2. \quad (17)$$

From Eqs. (15)–(17), we obtain

$$\sum_i |\nabla_i |\psi|^2| / |\psi|^4 = \left\{ \frac{1}{|\varphi_F|^2} \frac{d|\varphi_F|^2}{dr_{lm}} \right\}^2 = \left(\frac{d}{dr_{lm}} \ln |\varphi_F|^2 \right)^2. \quad (18)$$

Replacing φ_F with the expression (13), we finally have

$$\sum_i |\nabla_i |\psi|^2| / |\psi|^4 = 4 \left(\frac{1}{r_{lm}} + \frac{\eta}{a} \right)^2. \quad (19)$$

By inserting Eq. (19) into Eq. (10) and making use of Eq. (11), we obtain as the completed expression for $1/T_1$

$$\left(\frac{1}{T_1} \right)_s = \frac{8}{9} \frac{h}{\rho} \frac{\nu^3}{v^5} \coth \left(\frac{h\nu}{2KT} \right) I_s (I_s + 1) \nu_s^2 \times N_s r_{lm}^2 \left(\frac{1}{r_{lm}} + \frac{\eta}{a} \right)^2. \quad (20)$$

III. MAGNETIC CIRCULAR DICHROISM OF THE OPTICAL ABSORPTION BAND, AND THEORY OF ITS MEASUREMENT.

From fairly recent experimental^{15,8,17–20} and theoretical studies²¹ we have the following picture of the first-excited state of the F center in alkali halides. The appropriate wave function is essentially a hydrogenic P state which extends over several shells of ions surrounding the F -center vacancy. Orthogonalization of this P state to the ionic core orbitals leads to a large negative spin-orbit splitting; the splitting is especially due to the second shell of ions (halogens).

Qualitatively, selection rules for transitions to the excited state should be the same as those for the $1s \rightarrow 2p$ transition of hydrogen, as summarized in Fig. 2. However, even at low temperatures, the excited state exhibits a width of hundreds of cm^{-1} , and thus direct observation of the Zeeman effect is impossible. Nevertheless, because of the large spin-orbit splitting, the band is more or less separated into $P_{3/2}$ and $P_{1/2}$ parts. Thus, it is possible to observe large magnetic circular dichroism or Faraday rotation.

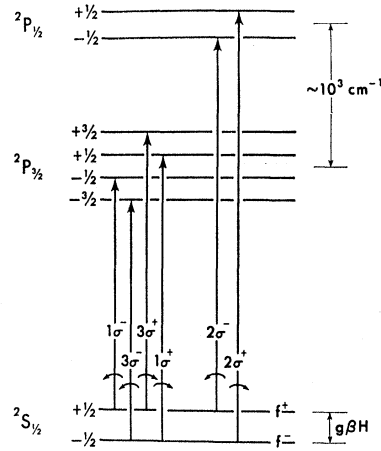


FIG. 2. Selection rules for the $S \rightarrow P$ absorption band of the F center. The Zeeman splittings shown are not resolved in the actual spectrum.

By magnetic circular dichroism, we mean differential absorption of σ^+ and σ^- circularly polarized light by the crystal, in the presence of a magnetic field H_0 . Furthermore, from the definition of σ^\pm , the light must be propagating parallel to H_0 . For transmitted and incident intensities I^\pm and I_0^\pm , respectively, of σ^\pm light we have the relation

$$I^\pm = I_0^\pm \exp[-l\gamma(\sigma^\pm)],$$

where l is the crystal thickness and γ the absorption coefficient per unit length. To facilitate analysis in terms of ground-state populations, we write

$$\gamma(\sigma^\pm) = f^+ \alpha(\sigma^\pm, +) + f^- \alpha(\sigma^\pm, -),$$

where $\alpha(\sigma^\pm, +)$ and f^+ are the fractional-absorption coefficient and fractional population for the ground-state sublevel $M_S = +\frac{1}{2}$, and $\alpha(\sigma^\pm, -)$ and f^- are the corresponding quantities for $M_S = -\frac{1}{2}$. We choose to measure a circular-dichroism signal defined by

$$S = 2(I^+ - I^-) / (I^+ + I^-) = \Delta I / I_{dc},$$

by switching the monitor beam rapidly between σ^+ and σ^- light. From the fact that the ground state is a Kramers' doublet, the absorption from that state must obey the symmetry $\alpha(\sigma^+, +) = \alpha(\sigma^-, -) \equiv \alpha^+$ and $\alpha(\sigma^+, -) = \alpha(\sigma^-, +) \equiv \alpha^-$. Under the assumptions that $S \ll 1$ and that $l[\gamma(\sigma^+) - \gamma(\sigma^-)] \ll 1$, it can be shown that

$$S(\lambda) = 2l\gamma_0(\lambda) \left\{ \frac{\alpha^+ - \alpha^-}{\alpha^+ + \alpha^-} \right\} P_e = KP_e, \quad (21)$$

where P_e is the ground-state electron-spin polarization $f^+ - f^-$, and where γ_0 is the absorption coefficient for $H_0 = 0$. K is a constant independent of H , and dependent primarily on the monitor wavelength λ , the crystal thickness, and the F -center concentration. K will be dependent on the temperature T only to the

¹⁷ F. Lüty and J. Mort, Phys. Rev. Letters **12**, 45 (1964).

¹⁸ R. Romestain and J. Margerie, Compt. Rend. **258**, 2525 (1964).

¹⁹ J. Margerie and R. Romestain, Compt. Rend. **258**, 4490 (1964).

²⁰ J. Gareyte and Y. Merle d'Aubigné, Compt. Rend. **258**, 6393 (1964).

²¹ D. Y. Smith, Phys. Rev. **137**, A574 (1965).

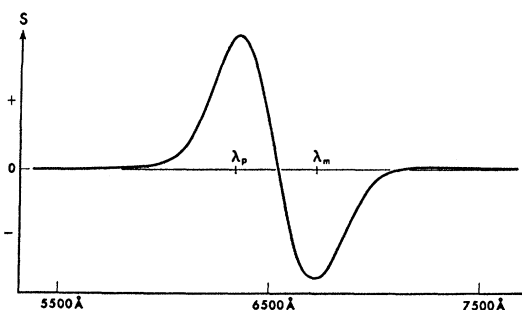


FIG. 3. Magnetic circular dichroism signal $S(\lambda)$ for the F center in KI at $H_0=10$ kG and $T=1.65^\circ\text{K}$. The quantities λ_p and λ_m are the pump and monitor wavelengths, respectively (see text).

extent that the absorption band is broadened and shifted at high temperatures.

In Eq. (21), the quantity $\Gamma \equiv \alpha^+ - \alpha^- / \alpha^+ + \alpha^-$, which we choose to call the "magnetic circular dichroism coefficient", is also a function of λ . From the relative transition probabilities shown in Fig. 2, it can be seen that if the spin orbit splitting effects a nearly complete separation of the $P_{3/2}$ and $P_{1/2}$ parts of the band, $\Gamma(\lambda)$ can be on the order of unity for the optimum wavelength. A large value of Γ is of course desired for good signal-to-noise ratio. Figure 3 shows a typical measurement of $S(\lambda)$ for the F center in KI at a fixed temperature and field; the curve is thus proportional to the product $\gamma_0(\lambda)\Gamma(\lambda)$.

A large value of Γ is also of great importance for optical pumping of the electron spins with circularly polarized light. That is, if one assumes equal probability for return to the ground state, then Γ represents the value of $-P_e$ to be obtained for saturated pumping with σ^+ light of a given wavelength. For further details and the appropriate rate equations see Ref. 22.

IV. EXPERIMENTAL

A block diagram of the apparatus is given in Fig. 4. For most of the experiments described below, the magnetic field was provided by the small superconducting solenoid shown; for fields of less than ~ 0.7 kG, the superconducting magnet was replaced by a copper

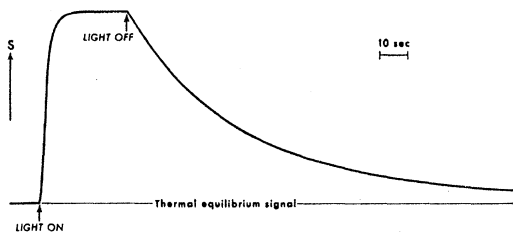


FIG. 4. Buildup of dichroism signal with optical pumping and decay back to thermal equilibrium. The very clean curve reflects the excellent signal to noise ratio attainable with optical detection; the decay curve is accurately exponential. ($H_0=800$ G.)

²² C. D. Jeffries, Phys. Rev. Letters 19, 1221 (1967).

Helmholtz coil external to the Dewar. The samples, typically about $5 \times 5 \times 1$ mm thick, were centered in the magnet bore where they could intercept the monitor beam propagating parallel to H_0 . Both sample and magnet were subject to the same He bath at 1.65°K .

The monitor beam consisted of a very narrow band of wavelengths centered about $\lambda_m=6800$ Å for KI and $\lambda_m'=6328$ Å for KBr. (See Fig. 3). The beam was switched from σ^+ to σ^- light by a vibrating quarter-wave plate of fused silica dynamically stressed at its mechanical resonance frequency of 16.7 kHz by piezoelectric transducers. The modulator and its proper adjustment have been fully described elsewhere.²³

To allow measurement of very small dichroism signals, the monitor-beam optics were carefully purged of all spurious circular dichroism. In the first place, all optical elements between the modulator and the sample had to be free of rotation; in this connection, the Dewar windows were of a special strain-free design, also described elsewhere.²⁴ Furthermore, all optical elements following the sample were such that no one linear polarization was favored over any other. Thus, it was necessary, for example, to use total internal reflection in a right-angle prism to turn the monitor-beam direction by 90° .

With the above precautions, it was possible to reduce the residual signal (that obtained with no sample or equivalently, that obtained at $H_0=0$) to an immeasurable level. That is, the residual signal, if any, represented a modulation of the transmitted intensity of considerably less than one part in 10^6 . Furthermore, I_{dc} corresponded to a flux of about 10^{10} to 10^{11} photoelectrons per second. For the above two reasons, it was possible to measure circular-dichroism signals as small as one part in 10^6 when the lock-in integration time was 1 sec.

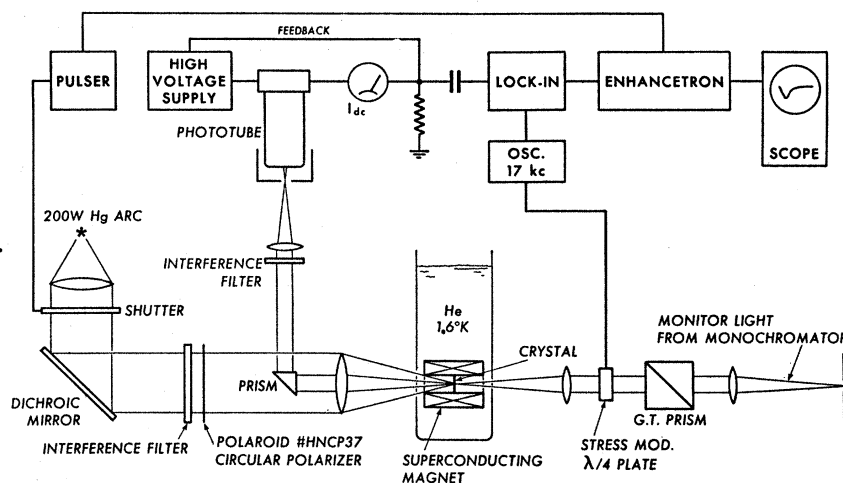
To facilitate the measurement of small changes in a large dichroism signal, it was necessary to stabilize I_{dc} against low-frequency noise sources, such as flicker of the xenon lamp supplying the monochromator. This stabilization was accomplished by means of a servo loop in which the photomultiplier tube power-supply voltage was controlled by I_{dc} itself. The feedback loop contained a single-time constant of the smallest value such that the feedback would produce no measurable effect on the 16.7-kHz dichroism signal. Thus, a great deal of correction was provided against noise components whose frequencies were less than, say, a few hundred cycles per second.

To measure spin-lattice relaxation times, it was necessary to perturb P_e from its thermal equilibrium value; this was accomplished by optical pumping with circularly polarized light from a 200-W Hg arc lamp. An interference filter limited the pump light to a narrow

²³ L. F. Mollenauer, D. Downie, H. Engstrom, and W. B. Grant, J. Appl. Opt. (to be published).

²⁴ L. F. Mollenauer, C. D. Grandt, W. B. Grant, and H. Panepucci, Rev. Sci. Instr. 39, 1958 (1968).

Fig. 5. Block diagram of the apparatus.



band of wavelengths centered about $\lambda_p = 6300 \text{ \AA}$ for KI; a corresponding pump wavelength $\lambda_p' = 5800 \text{ \AA}$ was used for KBr (see Fig. 3). A complementary interference filter centered at λ_m or λ_m' and installed in front of the detector completed the separation of the beams.

As an alternative to optical pumping, it was also possible to obtain a large initial value of $|P_e|$ by raising H_0 to several tens of kG. The field could then be switched in a fraction of a second to the value at which the measurement was to be taken. This method was used only for H_0 in the low-field range where relaxation times were very long.

For the measurement of long times ($T_1 \gtrsim 5$ sec) the lock-in signal was read out directly by a chart recorder. A typical example of the data thus obtained is shown in Fig. 5. For shorter times ($T_1 \lesssim 5$ sec), consecutive signals were added in a Nuclear Data Enhancetron Model No. 1024 to improve the signal-to-noise ratio. The latter process was automated by means of a solenoid-actuated mechanical shutter in front of the pump lamp.

The samples were prepared from Harshaw crystals both by the method of additive coloration and by an electrolytic process. For the former, the crystals and a small quantity of potassium metal were sealed into an evacuated tube and baked at a temperature of 600°C for times on the order of 10 min or less. The method is treated in detail by Van Doorn.²⁵ In the latter, the crystals were subject to an electric field of a few hundred V/cm, again at a temperature of 600°C . To avoid the deleterious effects of oxygen and water vapor, the process was carried out in an atmosphere of nitrogen. The field was turned off when the current through the crystal had risen to a predetermined value, and the crystals quenched by rapid cooling to room temperature or lower. Although the sample properties at high magnetic field seemed to be independent of

sample-preparation technique, the longest relaxation times at low field were found for the electrolytically colored samples (see Sec. V). Since, in addition, the electrolytic process was easier to control, most of the samples were prepared by that method. The resulting F -center concentrations never exceeded $10^{16}/\text{cm}^3$, as determined by absolute measurement of absorption band strength.

Finally, a few details of the superconducting magnet should be of interest on account of its high performance and low cost. The magnet was designed and built in this laboratory. It was wound of uninsulated copper-clad Nb-Ti wire on a copper spool of approximately 40-mm length by 30-mm outside diam, and had an inner bore of 9 mm. The only insulation used was that provided by single layers of porous fiberglass cloth between winding layers. Despite its small size, the magnet could produce fields up to 55 kG at a current of 70 A; this performance corresponded very closely to that listed by the wire manufacturer for short samples. A simple but efficient heat exchanger on the current leads in the path of the He blow-off gas reduced the measured heat load on the He bath at full current to less than 300 mW.

Calibration of the magnet was by means of the Zeeman effect of the R_1 line of dilute ruby. The splitting scheme is well known from the analysis of Sugano and Tanabe,²⁶ and the pertinent g factors are known accurately from resonance experiments.^{27,28} The ruby sample, which was only $\frac{1}{4}$ mm thick in the direction parallel to its C axis, was mounted with that axis accurately parallel to H_0 . The R_1 -line fluorescence was analyzed by the modulator of Fig. 4 before it was passed through a high-resolution grating spectrometer and from there on to the detector. Thus, it was possible to resolve Zeeman splittings (between σ^+ and σ^- com-

²⁶ S. Sugano and Y. Tanabe, J. Phys. Soc. Japan 13, 880 (1958).

²⁷ J. E. Geusic, Phys. Rev. 102, 1252 (1956).

²⁸ S. Geschwind, R. J. Collins, and A. L. Schawlow, Phys. Rev. Letters 3, 545 (1959).

²⁵ Van Doorn, Rev. Sci. Instr. 32, 755 (1961).

ponents) at low field where they would not be resolved in the direct spectrum. At fields in the neighborhood of 50 kG, the splittings produced were more than one order of magnitude greater than the widths of the individual components. The magnet current was measured in terms of the voltage drop across a heavy manganin shunt and read out on a digital voltmeter. Thus, to within the accuracy of the above method, which is considerably better than 0.3% at high fields, we were able to show proportionality between H_0 and the magnet current for all fields up to the maximum. A calibration point near the maximum was used in setting the digital voltmeter to read the field directly in G.

V. RESULTS AND DISCUSSION

The principal experimental results are summarized in Fig. 6. The solid curves are of the form

$$1/T_1 = (AH^3 + BH^5) \coth(g\beta H/2KT), \quad (22)$$

where $(T)^{-1}$ is in sec^{-1} , H is in G, and where the parameters A and B have been determined from a computer-generated least-squares fit of expression (22) to the experimental points. In the fitting, all data points below $H=5$ kG were thrown out, as the behavior in this region is similar to that observed in Refs. 2 and 6, which was shown to be due to clusters of F centers.^{2,7} Since the relaxation rates span several orders of magnitude in the region of interest, the fitting was based upon the fractional deviations of the experimental points from the theoretical curve. The values of A and B thus determined are given in Table I, where we have included an appropriate value of the parameter

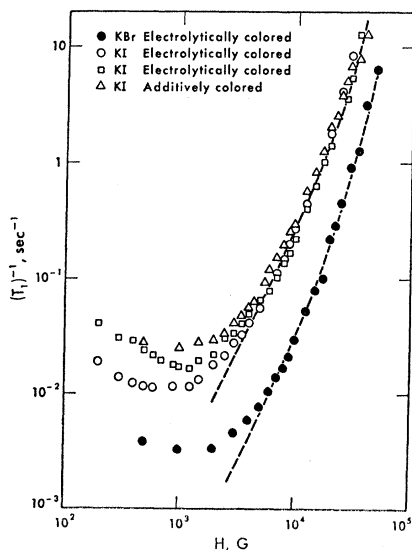


Fig. 6. Experimentally measured relaxation rates and fitted curves for the F center in KI and KBr (see text).

A for KCl from the data of Warren, Feldman, and Castle.⁶

The theoretical curves of Fig. 6 should be an accurate representation of the empirical behavior of the isolated F center. In the first place, the data points for samples prepared in different ways and of varying F -center concentration all converge closely in the high-field region. Furthermore, no field dependence is to be expected theoretically other than that given by the two terms of expression (22) for the hyperfine and Kronig mechanisms. For the determination of the parameters A and B , the least-squares fitting described above reduces the effects of random error by a very large factor when the number of data points is large. Finally, no significant systematic error is expected for the experimental technique used here.

We are now able to give precise expression to the qualitative statements made earlier about the relative importance of the two relaxation mechanisms. That part of the rate due to the hyperfine mechanism will be given by the fraction $A/(A+BH^2)$; this fraction is plotted in Fig. 7 as a function of H for both KI and KBr.

TABLE I. Values of the parameters A and B to make the curve $1/T_1 = (AH^3 + BH^5) \coth(g\beta H/2KT)$ fit the experimental points.

Crystal	A ($\text{sec}^{-1} \text{G}^{-3}$)	B ($\text{sec}^{-1} \text{G}^{-5}$)
KI	9.71×10^{-14}	10.0×10^{-23}
KBr	1.05×10^{-14}	1.68×10^{-23}
KCl	2.8×10^{-16}	

Theoretical values of the parameter A are given in Table II. In the computation of the theoretical rates, the values $v = (c_{44}/\rho)^{1/2}$ were chosen for the speed of sound, and the values of η used for KBr and KI represent extrapolations of values given in Ref. 15 for other alkali halides.

The values of ν_l were those determined by the ENDOR experiments of Seidel.¹⁰ A_1 and A_2 represent the contributions from the first and second shell of nuclei, respectively; no higher shells were found theoretically to make significant contribution. Thus, the total theoretical rate is given by $A = A_1 + A_2$. It is interesting to note that most of the hyperfine relaxation mechanism in KCl is contributed by the first shell, whereas the second predominates for KBr and KI. This shift in relative importance of the potassium versus the halogen nuclei is due primarily to the large nuclear magnetic moments of Br and I.

The last column of Table II compares theory to experiment. In view of the many approximations that had to be made in the calculation, the agreement in absolute value is about as good as could be reasonably expected. However, in judging the correctness of the theory, it is of much greater significance that the ratio

TABLE II. The parameters *A* as computed theoretically from expression (20), and comparison with *A* experimental. The values of important parameters appearing in (20) are included.

Crystal	$v^5/10^{25}$ (cm/sec) ⁵	η	ν_1 MHz	ν_2 MHz	$A_1/10^{-17}$ sec ⁻¹ G ⁻³	$A_2/10^{-17}$ sec ⁻¹ G ⁻³	$A/10^{-17}$ sec ⁻¹ G ⁻³	$A_{\text{expt.}}/A_{\text{theor.}}$
KI	2.1	2.70	10.4	49.5	13.4	1170	1180	8.2
KBr	4.5	2.54	18.3	42.8	9.8	182	193	5.5
KCl	16.9	2.44	21	7.0	4.5	1.7	6.2	4.5

of experimental to theoretical rates is nearly constant as one goes from KCl to KI; this fact becomes especially significant when one realizes that the corresponding absolute rates span a range of roughly 300 to 1. That is, in view of the great similarities among *F* centers in the various crystals, it is likely that the absolute values will be in error by a common multiplicative factor arising primarily in the calculation of $\nabla|\psi|^2$. Nevertheless, the constancy of the ratios reflects the fact that the experimental values are scaling properly according to factors such as ν_1^2 and v^{-5} in expression (20). In view of the above agreement, we are left with little doubt that our theory is essentially correct.

The fact that our theoretical relaxation rates are smaller than those observed could be attributed to the neglect of the ion-ion overlaps in the wave function (12). Inclusion of such terms in Φ will make the electron density $|\psi|^2$ at a given nucleus depend upon the mutual displacements of all the others; this will have the effect of allowing the phonons more opportunity to act upon the electron spin. The preceding argument could explain the somewhat too fast relaxation rates obtained in Ref. 14 for KCl where the authors have overestimated the mutual dependence by using molecular orbital-type wave functions for the *F* electron.

Unfortunately, no proper calculation of the Kronig mechanism is yet available for the *F* center. However, in his original paper,¹² Kronig treated a problem similar in most respects except for the detailed nature of the wave functions. Thus, in addition to yielding the exact field dependence, Kronig's expression for the relaxation rate should also indicate, at least approximately, the proper dependence upon the spin-orbit splitting δ and the energy of the first excited state Δ relative to the ground state. The expression should also yield a very crude order-of-magnitude agreement in absolute value between calculated and experimentally determined

TABLE III. Values of the parameter *B* computed from expression (23), and comparison with *B* experimental. Some parameters entering into the calculation of *B* theoretical have been included for convenient reference.

Crystal	δ/Δ	Δ , cm ⁻¹	$B_{\text{theor.}}$	$B_{\text{theor.}}/B_{\text{expt.}}$
KI	15.8×10^{-3}	15 300	24×10^{-22}	24.0
KBr	9.1×10^{-3}	16 800	4.1×10^{-22}	24.4
KCl	4.7×10^{-3}	20 600	3.6×10^{-23}	...

rates. In a slightly modified form, Kronig's expression is

$$\frac{1}{T_1} = -\frac{3}{4} \frac{1}{\pi^2 \hbar^4} \left(\frac{e^4}{\rho a^2} \right) \left(\frac{g\beta}{v} \right)^5 \left(\frac{\delta}{\Delta} \right)^2 \frac{1}{\Delta^2} \times H^5 \coth \frac{g\beta H}{2KT}, \quad (23)$$

where *a* is the lattice constant and *e* is the electronic charge. Table III gives the values of the parameters *B* calculated for KBr and KI from expression (23), and compares them to the experimentally determined parameters *B* of Table I. Although the intercomparison would be more meaningful if data were also available for KCl, at least it can be seen from the above that in the comparison of KBr to KI, the theoretical rates are in the same ratio as the experimentally determined ones. As for the very rough correspondence in absolute rates, one can at least be assured that the Kronig mechanism is capable of providing an effect of the size observed. In view of the simplicity of the *F* center and its consequent amenability to theoretical treatment, and in view of the fact that accurate experimental data are now available, a proper calculation of the Kronig mechanism for the alkali halides should be most rewarding. Until such computation is made, our contention that the behavior at very high fields is due to the Kronig mechanism must rest primarily upon the very close conformity of the experimentally determined field dependence to the theoretical behavior $T_1^{-1} \propto H^5 \coth(g\beta H/2KT)$.

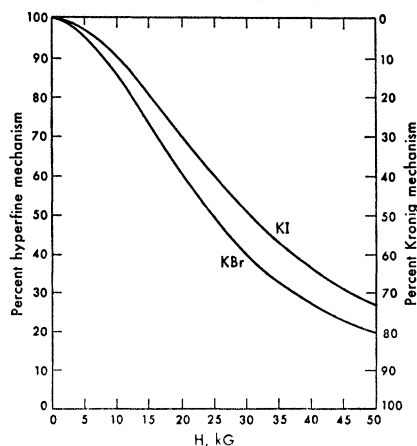


Fig. 7. Percent of relaxation rate due to hyperfine and Kronig mechanisms as a function of H_0 .

VI. APPLICATION TO OPTICAL PUMPING OF NUCLEAR SPINS

The original aim of this work was to elucidate several questions concerning the applicability of the nuclear polarization schemes proposed by Jeffries²² to F centers. For systems exhibiting hyperfine contact interaction between paramagnetic electrons and nuclei, these schemes involve polarization of the electrons by optical pumping, and transfer of this polarization to the nuclei through selective relaxation between hyperfine levels. Although a complete discussion of the optical-pumping problem is beyond the scope of this paper, it is nevertheless fitting that we point out briefly how the principal results of the work apply to that problem.

First, our optical-pumping experiments established that with easily attainable light intensities, it was possible to completely overwhelm the spin-lattice relaxation rate, and thus to obtain saturated pumping of the electron spins for H_0 in the following ranges: $0 < H_0 \lesssim 5$ kG for KI and $0 < H_0 \lesssim 7$ kG for KBr. Our criterion for saturation was that the value of P_e obtained for pumping with σ^+ light be equal in magnitude (but opposite in sign) from that obtained for pumping with σ^- . The saturated values of $|P_e|$ thus obtained were 40% and 12% for KI and KBr, respectively; these values should be equal to the magnetic circular-dichroism coefficient Γ of Sec. IV. From absolute measurements of the dichroism,^{8,20} one can compute values of Γ that are in good agreement with the above results. It is also of some interest to note the values of field at which optical pumping in opposition to the relaxation was just able to bring P_e to zero; these values were $H_0 = 15.6$ kG and $H_0 = 18$ kG for KI and KBr, respectively. The above results are rather sensitive to the spectral characteristics of the pump lamp and could be altered significantly with use of other pump sources.

As an intermediate step in the polarization of nuclei distant from the F center, it is necessary to polarize the nuclei making direct contact with the F -center electron; most effective here would be the 12 equivalent halogen nuclei of the second shell. From our study of the relaxation mechanism, we may be reasonably certain that under the proper conditions, the contact interaction nuclei will be polarized with optical pumping. For that range of field H_0 where the hyperfine relaxation mechanism is dominant, the pertinent relaxation operators are I^+S^- and I^-S^+ , i.e., the nucleus must always undergo a change $\Delta M_I = -\Delta M_S = \pm 1$. Now, suppose the optical pumping tends to put a majority of the F centers into the $M_S = +\frac{1}{2}$ set of hyperfine levels. All of these will be able to relax except the level $M_I = +I$. The net result of a number of

pumping cycles will then be to allow buildup of population in that hyperfine level, and thus the contact nuclei will tend to become polarized.

On the other hand, for relaxation by the Kronig mechanism, the pertinent selection rule is $\Delta M_I = 0$. Thus, the nuclear spin pumping described above will tend to be destroyed by Kronig relaxation, and hence we would expect the polarization of contact nuclei to disappear at very high field. Similar arguments may also apply for relaxation by the "extrinsic effects" seen at low fields. But for fields in the range of, say, $5 \text{ kG} \lesssim H_0 \lesssim 15 \text{ kG}$, where neither of these mechanisms is important relative to the hyperfine mechanism, optical pumping of the contact nuclei may well be rather efficient.

If the contact nuclei are indeed polarized, it may then be possible to transfer this polarization to distant halogen nuclei through spin diffusion or through cross relaxation. To detect the polarization, one would perform a standard NMR experiment on the distant nuclei and compare signal intensities with and without optical pumping of the F center. The range of field for which such an effect is most likely is that indicated in the above paragraph; especially effective here may be a cross relaxation point between the distant and contact iodine nuclei in KI which occurs at 14.65 kG. We have not yet performed such an experiment in the appropriate field range for lack of a suitable magnet. Previous to this study, we did attempt to see the effects of optical pumping at very low fields, but with negative results. However, according to our study of the spin-lattice relaxation, these first unsuccessful attempts in no way preclude the possibility of positive results at higher field.

ACKNOWLEDGMENTS

Above all, we would like to acknowledge our manifold debt to C. D. Jeffries. In the first place, this investigation had its origin in his suggestion that we attempt to polarize nuclei by optical pumping of F centers. Secondly, both of us owe our understanding of spin-lattice relaxation to the patient tutoring of Jeffries in this subject. Finally, the many discussions we have had with him during the preparation of this manuscript have been invaluable. We also gratefully acknowledge the careful and meticulous work of H. Engstrom in calibrating the magnet, as well as engineering assistance given us by R. Hintz in producing the coil. Quite a number of magnets built according to Hintz's technique have been very successful. We are indebted to the Consejo Nacional de Investigaciones Cientificas y Tecnicas, Argentina for helping make possible Panepucci's stay in Berkeley.